

Supporting Information

The role of zero-field splitting and π -stacking interaction of different nitrogen-donor ligands on the optical properties of luminescent rhenium tricarbonyl complexes

Plinio Cantero-López^{1,2*}, Yoan Hidalgo-Rosa^{3,4}, Zoraida Sandoval-Olivares³, Julián Santoyo-Flores³, Pablo Mella^{3,5}, Lily Arrué³, César Zúñiga^{6,7}, Ramiro Arratia-Pérez^{1,2*}, Dayán Páez-Hernández^{1,2*}

¹Center of Applied Nanoscience (CANS), Facultad de Ciencias Exactas, Universidad Andres Bello, Av. República 330, Santiago, Chile.

²Relativistic Molecular Physics (ReMoPh) Group, Ph.D. Program in Molecular Physical Chemistry, Universidad Andres Bello, Av. República 275, Santiago, Chile.

³Doctorado en Fisicoquímica Molecular, Universidad Andres Bello, Ave. República #275, Santiago de Chile, Chile.

⁴ANID – Millennium Science Initiative Program- Millennium Nuclei on Catalytic Process towards Sustainable Chemistry (CSC), Chile.

⁵Universidad Andres Bello, Facultad de Ciencias Exactas, Departamento de Ciencias Químicas, Quillota 980, Viña del Mar, Chile.

⁶ Instituto de Ciencias Naturales, Facultad de Medicina Veterinaria y Agronomía, Universidad de Las Américas, Sede Providencia, Manuel Montt 948, 7500972 Santiago, Chile.

⁷Facultad de Ciencias de la Salud, Universidad Central de Chile, Lord Cochrane 417, Santiago, Chile.

Electron localization function (ELF)

The electron localization function (ELF)¹ was used as a quantum-mechanical method for the characterization of the metal–ligand bonding^{2,3}. **Figures S4 and S5** showed the corresponding 2D plots of ELF and the electron density (ρ) contours, located between rhenium and nitrogen atoms from denitrogenated ligands (N,N).

As represented in **Figures S4 and S5**, there are disynaptic valence and core basin around Re(I) and N/C atoms. The ELF values near the nuclei were much less than 1, indicated that the bond was not purely ionic. Therefore, it was proved to be a strong evidence of covalent bond character around the metal center. This was also confirmed by ELF values in the interstitial region, which were less than 0.2, but never zero. **Figures S4 and S5** (see supporting information) also showed that the BCP values for C-C bonds are located at the midpoint, meanwhile in N–C bonds, it was shifts away from the geometrical center toward the C atom. This gave evidence of the polarization that existed in this bond, which in turn played an important role in the charge transfer phenomena, from the metal to ligand, involving in the excited states ,also $d\pi \rightarrow \pi^*$ interactions were similar as discussed in the optical properties section.

Natural Bond Orbital (NBO) Analysis

To finally complement the study of the selected complexes Natural Bond Orbital analysis (NBO) was also performed. The calculated natural atomic charges (NAC) of the rhenium and nitrogen atoms have been listed in **Table S3** (see supporting information). This analysis showed that the charge reduction in the metal center was lower than the formal charge (+1). This was resultant of a significant charge donation from ancillary ligands, particularly chlorine and nitrogen atoms directly bound to the first coordination sphere. The calculated NAC over N-donor center was smaller and less negative than the charge on the Cl atom. I, which indicated that there was higher electron density delocalization from the N-donor center to rhenium. The fact is well described and supported by literature,^{4,5} that each natural bond orbital (NBO) σ_{AB} can be expressed in terms of two directed valence hybrids (NHOs) h_A and h_B on atoms A and B such as:

$$\sigma_{AB} = c_A h_A + c_B h_B \quad (1)$$

Here, cA and cB are the polarization coefficients. The corresponding valence anti-bonding NBO must be:

$$\sigma_{AB}^* = c_A h_A - c_B h_B \quad (2)$$

As shown in **Table S3**, NBO analysis for the complexes under study confirmed the bond orbital for all Re–N bonds. Additionally, s, p and d orbitals of rhenium participate in the formation of Re–N bond. With a higher d character ($\geq 75\%$ approximately). The p contribution is the most important in the nitrogen atom ($\geq 80\%$ approximately). In the systems with monodentate triazole ligands, the $d\pi \rightarrow \pi$ donations from Re to N atom were observed, as well as in the dinitrogenated ligands, confirming the π acceptor character in these ligands. Therefore, the compounds under the introduction of two nitrogen-donor ligand the π acceptor character increase, which in turn could help to explain the higher values in the ZFS parameter observed in these complexes.⁶

References

- 1 A. Savin, R. Nesper, S. Wengert and T. F. Fässler, *Angew. Chemie (International Ed. English)*, 1997, **36**, 1808–1832.
- 2 P. Jerabek, B. Von Der Esch, H. Schmidbaur and P. Schwerdtfeger, *Inorg. Chem.*, 2017, **56**, 14624–14631.
- 3 M. Duan, P. Li, H. Zhao, F. Xie and J. Ma, *ACS Publ.*, 2019, **58**, 3425–3434.
- 4 R. Kia and A. Kalaghchi, *Crystals*, 2020, **10**, 267.
- 5 S. Michalik, B. Machura, R. Kruszynski and J. Kusz, *J. Coord. Chem.*, 2008, **61**, 1066–1077.
- 6 M. C. Barral, D. Casanova, S. Herrero, R. Jiménez-Aparicio, M. R. Torres and F. A. Urbanos, *Chem. - A Eur. J.*, 2010, **16**, 6203–6211.

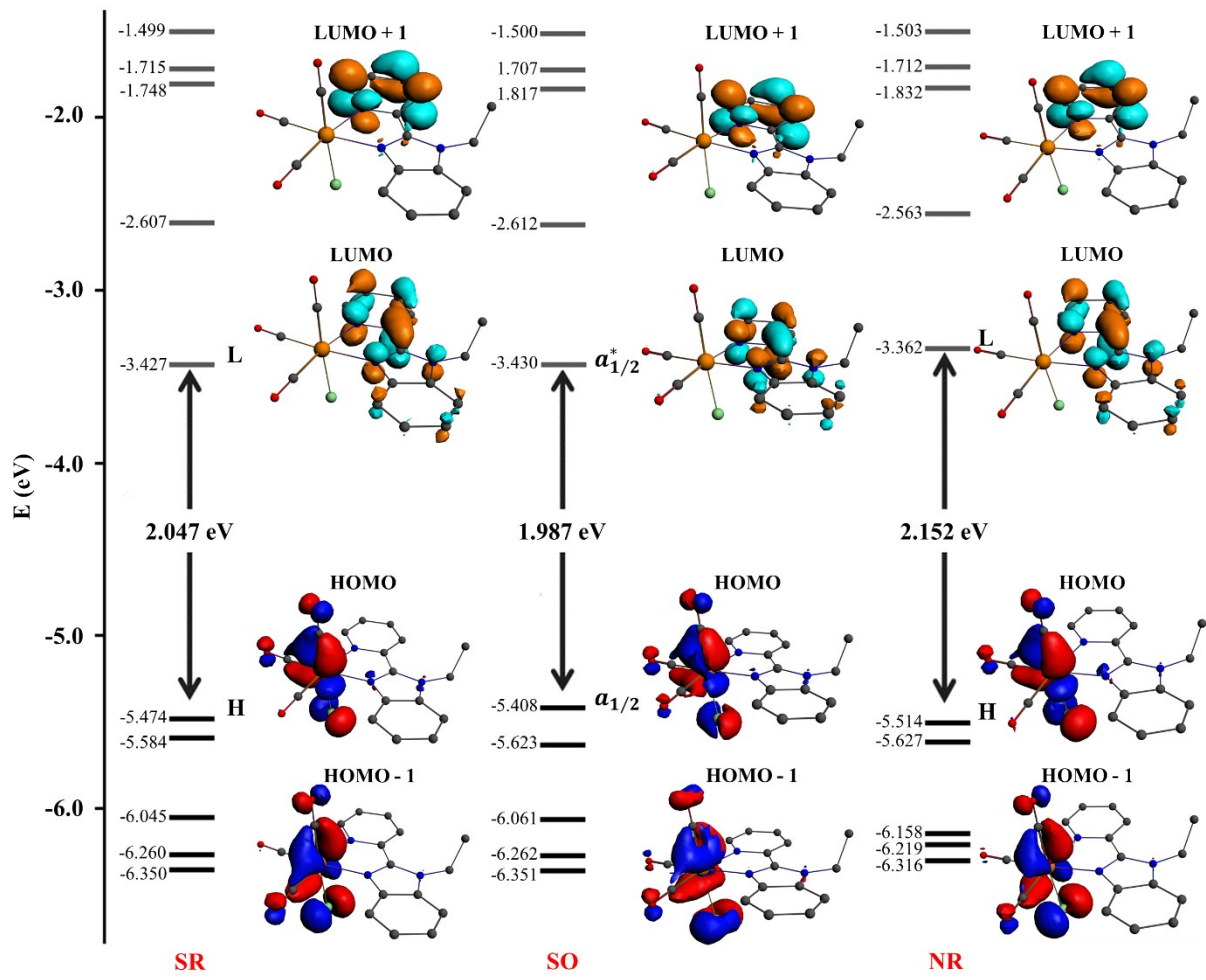


Figure S1. Energy levels and MOs isosurface diagrams of compound number 5 at the BP86 level

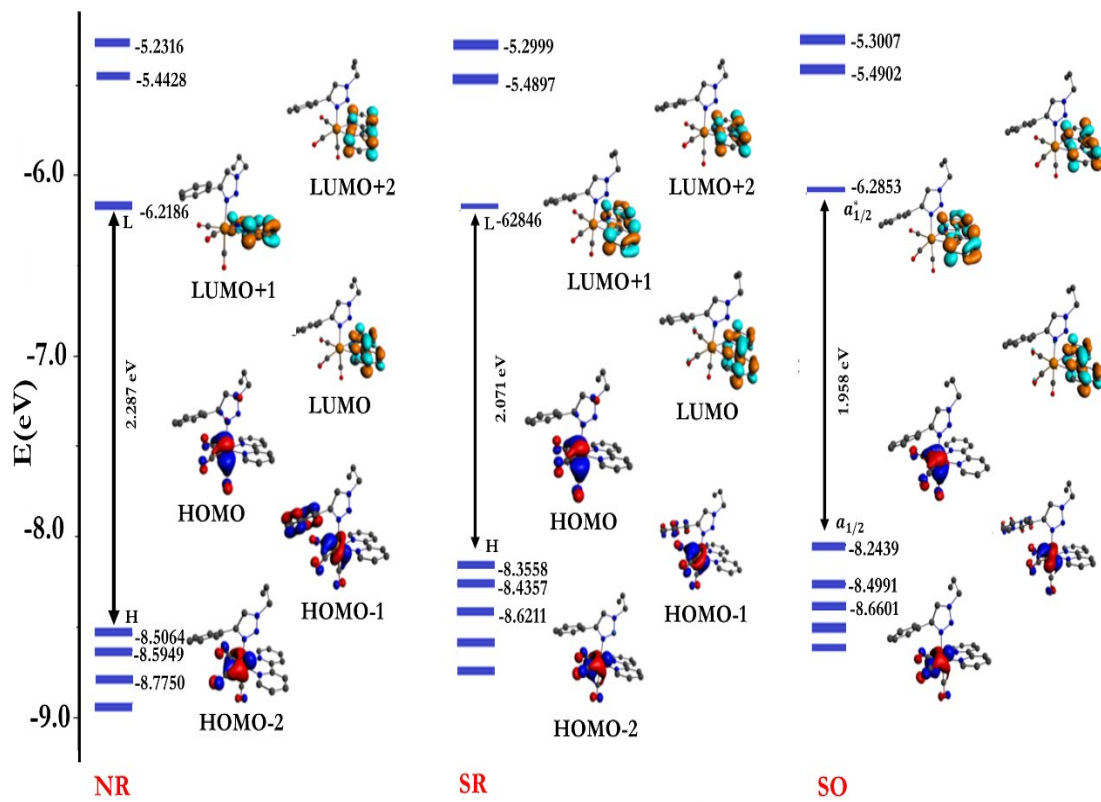


Figure S2. Energy levels and MOs isosurface diagrams of compound number 4 at the BP86 level

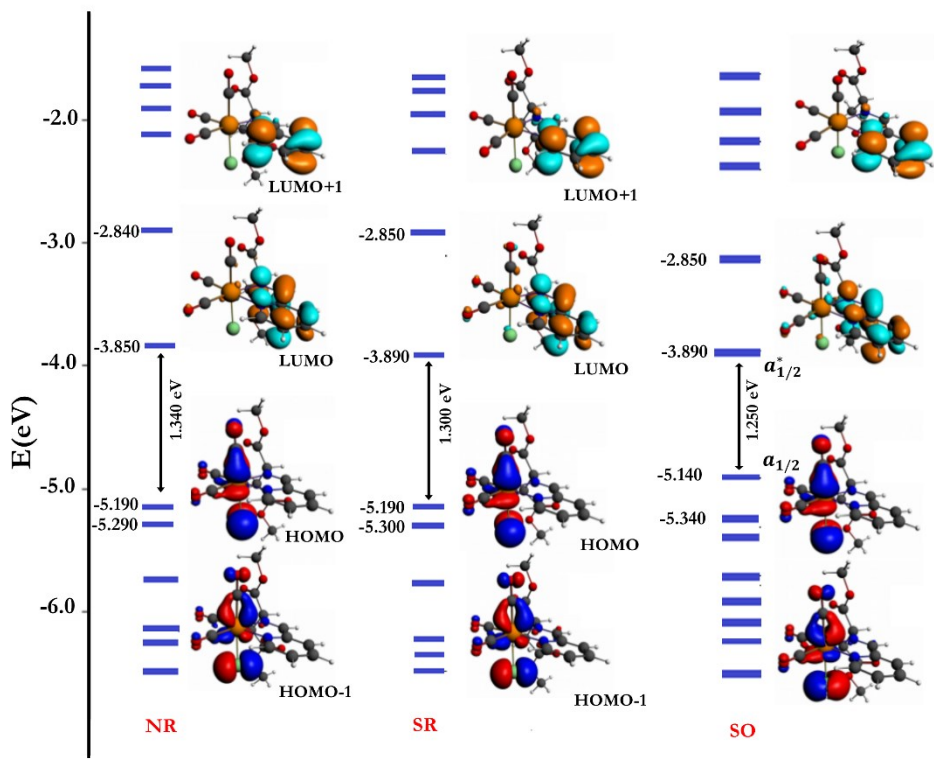
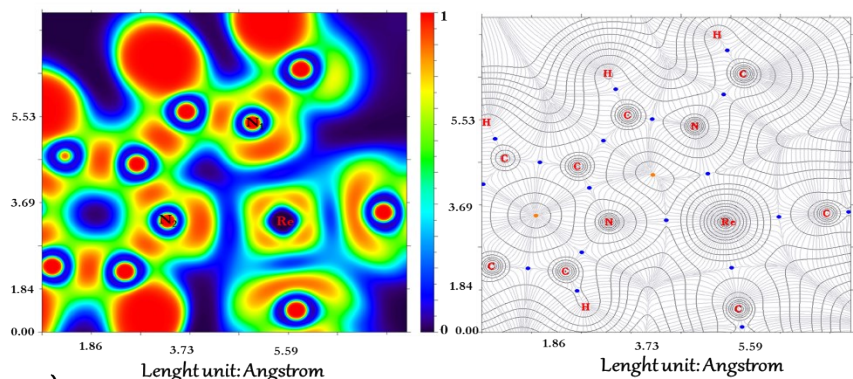
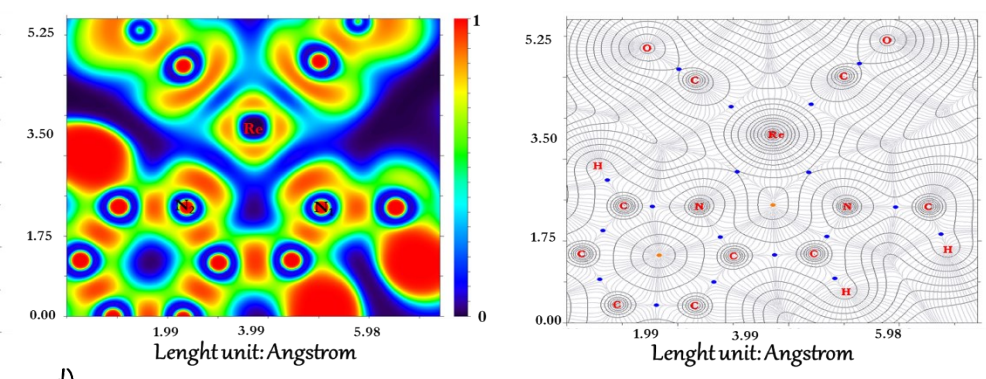


Figure S3. Energy levels and MOs isosurface diagrams of compound number 2 at the BP86 level

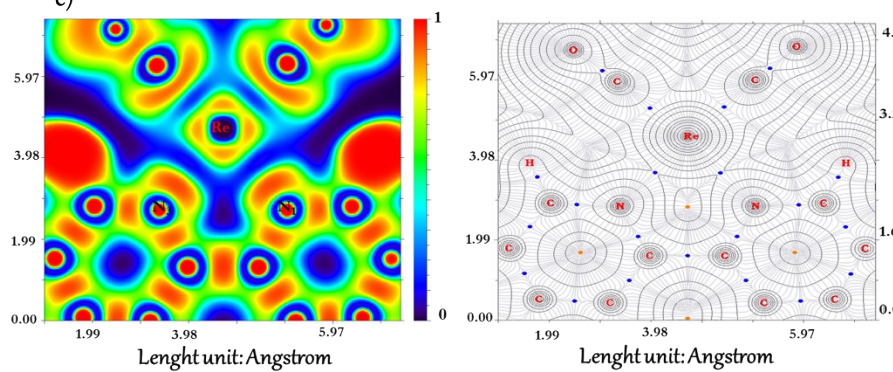
a)



b)



c)



d)

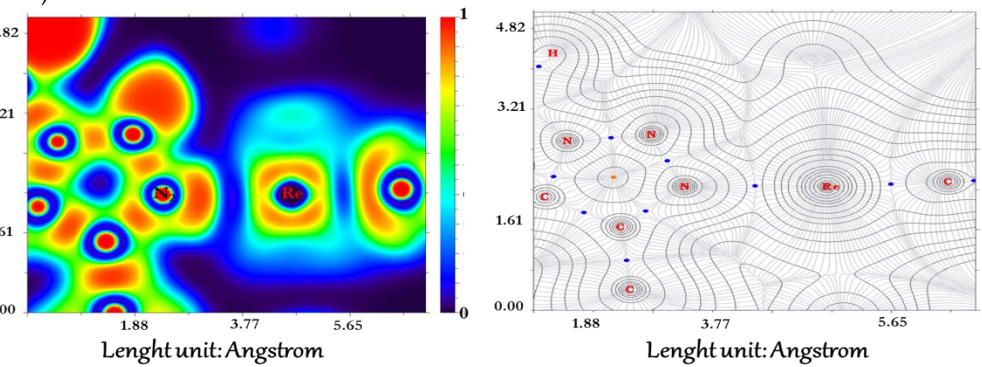


Figure S4. Contour plots of the electron localization function (ELF) and electron density $\rho(r)$ for: a) 1 b) 2 c) 3 (Intersecting plane:Re,N₁,N₃) d) 3(Intersecting plane:Re,N₂)

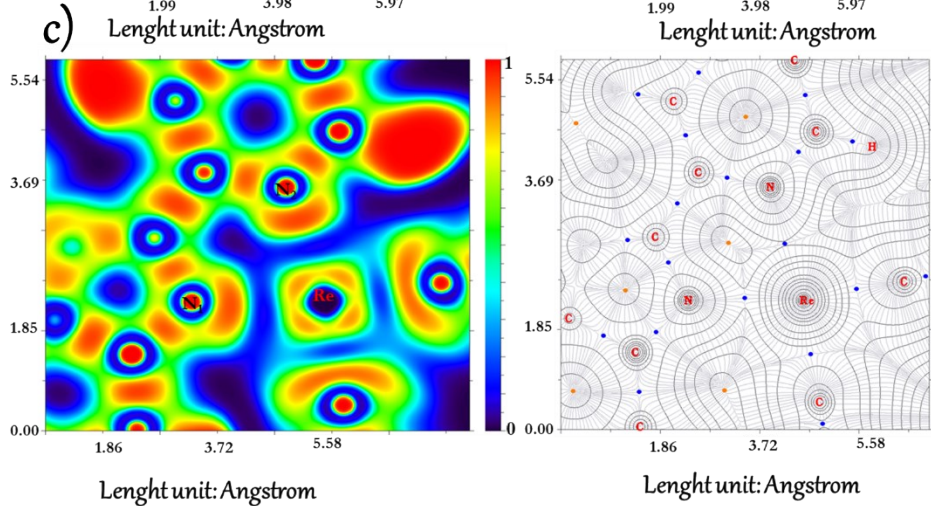
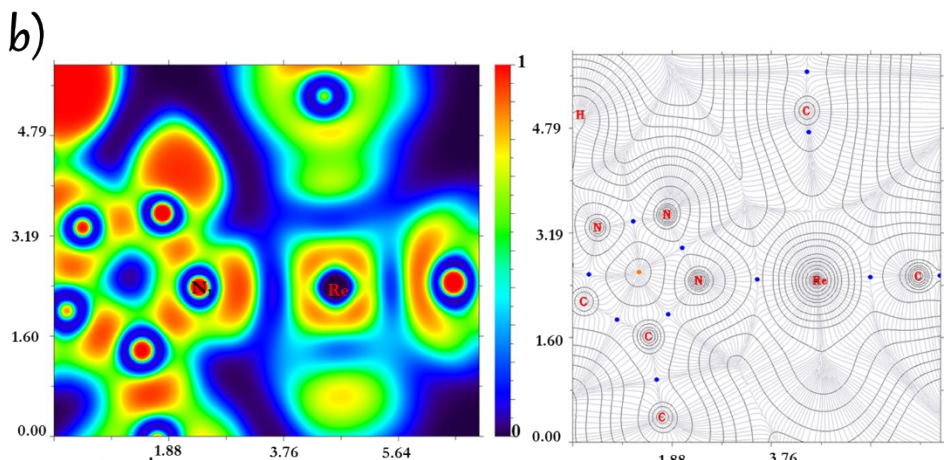
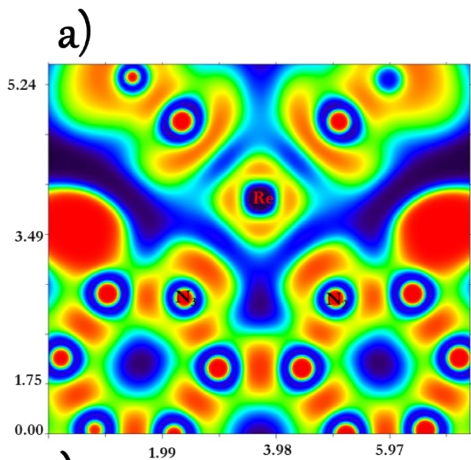


Figure S5. Contour plots of the electron localization function (ELF) and electron density $\rho(r)$ for: a) 4 (Intersecting plane:Re,N₁,N₂) b) 4 (Intersecting plane:Re,N₃) c) 5

Table S1. Optimized geometries for the ground state (S_0) of the luminescent rhenium tricarbonyl complexes. All distances are in angstrom (\AA)

Bond	NR	SR	SO	Literature	WBI
1					
Re–N ₁	2.192	2.201	2.159	2.178	1.132
Re–N ₂	2.224	2.191	2.189	2.176	1.143
Re–C ₁	1.961	1.922	1.921	1.910	1.317
Re–C ₂	1.969	1.932	1.931	1.924	1.313
Re–C ₃	1.962	1.926	1.925	1.917	1.318
Re–Cl	2.451	2.473	2.472	2.482	0.801
Re–N ₁ –N ₂ –Cl			85.464		
Angle					
C=O	1.146	1.143	1.140	1.156	
<i>v</i> (CO) <i>sym</i>		2024		2025	
<i>v</i> (CO) <i>asym</i>		1955		1925	
2					
Re–N ₁	2.219	2.190	2.186	2.187	1.130
Re–N ₂	2.217	2.183	2.182	2.170	1.134
Re–C ₁	1.960	1.924	1.923	1.952	1.193
Re–C ₂	1.961	1.921	1.920	1.992	1.184
Re–C ₃	1.967	1.993	1.932	1.897	1.183
Re–Cl	2.450	2.476	2.474	2.456	0.807
Re–N ₁ –N ₂ –Cl			59.093		
Angle					
C=O	1.157	1.161	1.161	1.139	
<i>v</i> (CO) <i>sym</i>		2007		2028	
<i>v</i> (CO) <i>asym</i>		1939		1928	
3					
Re–N ₁	2.207	2.189	2.188	2.17	1.131
Re–N ₂	2.250	2.245	2.243	2.21	1.132
Re–N ₃	2.204	2.187	2.186	2.17	1.136
Re–C ₁	1.962	1.921	1.920	1.92	1.308
Re–C ₂	1.952	1.918	1.917	1.91	1.316
Re–C ₃	1.962	1.924	1.923	1.93	1.314
Re–N ₁ –N ₂ –N ₃			54.968		
C=O	1.159	1.165	1.165	1.150	
<i>v</i> (CO) <i>sym</i>		2028		2035	
<i>v</i> (CO) <i>asym</i>		1960		1921	
4					
Re–N ₁	2.234	2.234	2.233	2.236	1.128
Re–N ₂	2.205	2.185	2.185	2.164	1.130
Re–N ₃	2.208	2.182	2.181	2.170	1.134
Re–C ₁	1.965	1.931	1.932	1.915	1.317
Re–C ₂	1.961	1.923	1.924	1.922	1.313
Re–C ₃	1.975	1.934	1.935	1.930	1.315
Re–N ₁ –N ₂ –N ₃			55.108		
Angle					
C=O	1.158	1.160	1.160	1.155	
<i>v</i> (CO) <i>sym</i>		2026		2035	
<i>v</i> (CO) <i>asym</i>		1931		1923	
5					

Re–N ₁	2.228	2.209	2.208	2.184	1.189
Re–N ₂	2.186	2.161	2.159	2.129	1.124
Re–C ₁	1.959	1.919	1.918	1.840	1.130
Re–C ₂	1.962	1.922	1.922	1.848	1.332
Re–C ₃	1.948	1.909	1.908	1.92	1.316
Re–Cl	2.469	2.502	2.501	2.475	0.822
Re–N ₁ –N ₂ –Cl			60.491		
C=O	1.160	1.169	1.170	1.131	
<i>v</i> (CO)sym		1996			
<i>v</i> (CO)asym		1994			

*The complexes were optimized in the solvent used experimentally to determine the optical properties via the COSMO model

*NR=non-relativistic , SR= scalar relativistic, SO= spin-orbit, WBI= Wiberg bond index

Table S2. Optimized geometries for the corresponding luminescent states (S₁,T₁) of the rhenium tricarbonyl complexes. All distances are in angstrom (Å).

Bond	S ₀	S ₁	T ₁	Luminescence Behavior
1				
Re–N ₁	2.201	2.227		
Re–N ₂	2.191	2.224		Fluorescence
Re–C ₁	1.922	1.942		
Re–C ₂	1.932	1.938		
Re–C ₃	1.926	1.938		
Re–Cl	2.473	2.403		
2				
Re–N ₁	2.190	2.247		
Re–N ₂	2.183	2.223		Fluorescence
Re–C ₁	1.924	1.925		
Re–C ₂	1.921	1.940		
Re–C ₃	1.993	1.946		
Re–Cl	2.476	2.385		
3				
Re–N ₁	2.189		2.138	
Re–N ₂	2.245		2.126	Phosphorescence
Re–N ₃	2.187		2.239	
Re–C ₁	1.921		1.945	
Re–C ₂	1.918		1.943	
Re–C ₃	1.924		1.952	
4				
Re–N ₁	2.234		2.210	
Re–N ₂	2.185		2.125	Phosphorescence
Re–N ₃	2.182		2.124	
Re–C ₁	1.931		1.965	
Re–C ₂	1.923		1.955	
Re–C ₃	1.934		1.963	
5				
Re–N ₁	2.209		2.183	

Re–N ₂	2.161	2.077	Phosphorescence
Re–C ₁	1.919	1.930	
Re–C ₂	1.922	1.973	
Re–C ₃	1.909	1.944	
Re–Cl	2.502	2.447	

*The use of S1 and T1 for the luminescent states was a formalism to better understand the photophysical behavior of the complexes, because normally the excited SO states cannot be classified as singlets or triplets because of their highly mixed-spin characters.

Table S3. HOMO-LUMO Gap for NR (No Relativistic), SR (Scalar Relativistic) and SO (Spin-Orbit) calculations.

Molecule	Gap
1	1.418 eV (NR), 1.371 eV (SR), 1.317 eV (SO)
2	1.340 eV (NR), 1.300 eV (SR), 1.250 eV (SO)
3	2.504 eV (NR), 2.720 eV (SR), 2.391 eV (SO)
4	2.287 eV (NR), 2.071 eV (SR), 1.958 eV (SO)
5	2.152 eV (NR), 2.047 eV (SR), 1.987 eV (SO)

Table S4. The occupancies, hybridization, and natural atomic charges (NACs) for the rhenium complexes in a NBO scheme.

BD	Oc. ^a	Hybridization of NBO	BD*	Oc. ^a	Atom	NAC
1						
Re-N ₁	1.984	0.6396 (spd)Re + 0.7687 (sp)N	0.7687 (spd)Re - 0.6396 (sp)N	0.032	Re	0.0408 4
Re-N ₁	1.711	0.6091 (spd)Re + 0.7931 (sp)N	0.7931 (spd)Re - 0.6091 (sp)N	0.526	N ₁	0.3802 2
Re-N ₂	1.985	0.6428 (spd)Re + 0.7661 (sp)N	0.7661 (spd)Re - 0.6428 (sp)N	0.015	N ₂	0.3344 4
Re-N ₂	1.921	0.6296 (spd)Re + 0.7770 (sp)N	0.7770 (spd)Re - 0.6296 (sp)N	0.203	Cl	0.5420 5
2						
Re-N ₁	1.984	0.6306 (spd)Re + 0.7761 (sp)N	0.7761 (spd)Re - 0.6306 (sp)N	0.020	Re	0.0514 7
Re-N ₁	1.752	0.5989 (spd)Re + 0.8008 (sp)N	0.8008 (spd)Re - 0.5989 (sp)N	0.420	N ₁	0.3968

							8
Re-N ₂	1.983	0.6391 (spd)Re + 0.7692 (sp)N	0.7692 (spd)Re - 0.6391 (sp)N	0.016	N ₂	0.3730 9	-
Re-N ₂	1.911	0.6195 (spd)Re + 0.7850 (sp)N	0.7850 (spd)Re - 0.6195 (sp)N	0.227	Cl	0.5343 9	-
							3
Re-N ₁	1.977	0.6381 (spd)Re + 0.7699 (sp)N	0.6381 (spd)Re - 0.7699 (sp)N	0.043	Re	0.0688 4	-
Re-N ₁	1.711	0.5969 (spd)Re + 0.8023 (p)N	0.8023 (spd)Re - 0.5969 (sp)N	0.579	N ₁	0.4128 7	-
Re-N ₂	1.978	0.6387 (spd)Re + 0.7694 (sp)N	0.7694 (spd)Re - 0.6387 (sp)N	0.042	N ₂	0.2675 7	-
Re-N ₂	1.713	0.5967 (spd)Re + 0.8025 (sp)N	0.8025 (spd)Re - 0.5967 (sp)N	0.570	N ₃	0.4139 2	-
Re-N ₃	1.976	0.6756 (spd)Re + 0.7372 (sp)N	0.7372 (spd)Re - 0.6756 (sp)N	0.049			
Re-N ₃	1.893	0.6233 (spd)Re + 0.7820 (sp)N	0.7820 (spd)Re - 0.6233 (sp)N	0.744			
							4
Re-N ₁	1.980	0.6376 (spd)Re + 0.7704 (sp)N	0.7704 (spd)Re - 0.6376 (sp)N	0.035	Re	0.0661 7	-
Re-N ₁	1.731	0.6002 (spd)Re + 0.7998 (sp)N	0.7998 (spd)Re - 0.6002 (sp)N	0.530	N ₁	0.2738 9	-
Re-N ₂	1.980	0.6377 (spd)Re + 0.7703 (sp)N	0.7703 (spd)Re - 0.6377 (sp)N	0.035	N ₂	0.4165 5	-
Re-N ₂	1.728	0.6009 (spd)Re + 0.7993 (sp)N	0.7993 (spd)Re - 0.6009 (sp)N	0.531	N ₃	0.4118 7	-
Re-N ₃	1.983	0.6776 (spd)Re + 0.7355 (sp)N	0.7355 (spd)Re - 0.6776 (sp)N	0.048			
Re-N ₃	1.896	0.6264 (spd)Re + 0.7795 (sp)N	0.7795 (spd)Re - 0.6264 (sp)N	0.753			
							5
Re-N ₁	1.981	0.5098 (spd)Re + 0.8603 (sp)N	0.8603 (spd)Re - 0.5098 (sp)N	0.043	Re	0.0607 2	-
Re-N ₁	1.850	0.6155 (spd)Re + 0.7882 (sp)N	0.7882 (spd)Re - 0.6155 (sp)N	0.688	N ₁	0.4108 4	-
Re-N ₂	1.976	0.6378 (spd)Re + 0.7702	0.7702 (spd)Re -	0.029	N ₂	-	

		(sp)N	0.6378 (sp)N	0.3920	
				4	
Re-N ₂	1.705	0.5856 (spd) Re + 0.8106 (sp)N	0.8106 (spd)Re - 0.5856 (sp)N	0.657	Cl
				-	0.5283
				3	

^aOccupancy , BD denotes 2-center bond, * –denotes antibond NBO.

Table S5. Topological parameters of electron density derived from the Bader's theory of AIM: electron density ($\rho(r)$), Hessian eigenvalues, potential energy density $V(r)$, total energy densities $H(r)$ and lagrangian kinetic energy ($G(r)$) at the bond critical points (BCPs).

Bonds	$\rho(r)$	$V(r)$	$G(r)$	$H(r)$	$ V/G $
1					
Re–N ₁	0.0824	-0.1188	0.1023	-0.0665	1.1613
Re–N ₂	0.0817	-0.1197	0.1045	-0.0660	1.1455
Re–C ₁	0.1467	-0.2517	0.1955	-0.1249	1.2875
Re–C ₂	0.1414	-0.2413	0.1905	-0.1158	1.2667
Re–C ₃	0.1435	-0.2460	0.1936	-0.1177	1.2707
Re–Cl	0.0592	-0.0647	0.0561	-0.0362	1.1533
2					
Re–N ₁	0.0771	-0.1088	0.0944	-0.0605	1.1525
Re–N ₂	0.0781	-0.1130	0.0943	-0.0611	1.1983
Re–C ₁	0.1434	-0.2424	0.1898	-0.1200	1.2771
Re–C ₂	0.1450	-0.2393	0.1884	-0.1163	1.2702
Re–C ₃	0.1468	-0.2511	0.1945	-0.1252	1.2910
Re–Cl	0.0564	-0.0605	0.0526	-0.0326	1.1502
3					
Re–N ₁	0.0801	-0.1155	0.1007	-0.0630	1.1470
Re–N ₂	0.0803	-0.1158	0.1006	-0.0615	1.1511
Re–N ₃	0.0676	-0.0957	0.0867	-0.0487	1.1038
Re–C ₁	0.1402	-0.2407	0.1909	-0.1111	1.2609
Re–C ₂	0.1395	-0.2368	0.1876	-0.1123	1.2623
Re–C ₃	0.1398	-0.2365	0.1873	-0.1122	1.2627
4					
Re–N ₁	0.0812	-0.1175	0.1021	-0.0621	1.1508
Re–N ₂	0.0806	-0.1162	0.1012	-0.0636	1.1482
Re–N ₃	0.0698	-0.0092	0.0896	-0.0511	1.1071
Re–C ₁	0.1377	-0.2328	0.1847	-0.1118	1.2604

Re-C ₂	0.1410	-0.2410	0.1904	-0.1124	1.2658
Re-C ₃	0.1390	-0.2343	0.1861	-0.1134	1.2590
5					
Re-N ₁	0.0773	-0.1114	0.0979	-0.0608	1.1379
Re-N ₂	0.0843	-0.1217	0.1051	-0.0719	1.1579
Re-C ₁	0.1422	-0.2395	0.1880	-0.1191	1.2739
Re-C ₂	0.1418	-0.2396	0.1881	-0.1187	1.2738
Re-C ₃	0.1428	-0.2425	0.1894	-0.1197	1.2804
Re-Cl	0.0610	-0.0673	0.0582	-0.0380	1.1564

Table S6 . Cartesian coordinates of **1** at the ZORA/BP86/TZ2P level of theory.

Re	14.211600000	2.116580000	3.950320000
Cl	12.917530000	2.973910000	2.012910000
N	15.350890000	1.090810000	2.405520000
N	13.119280000	0.271690000	3.565480000
C	15.537680000	-0.948530000	1.158780000
C	13.641120000	-0.516270000	2.712190000
C	17.148420000	0.779150000	0.856130000
C	16.691660000	-0.492560000	0.550130000
C	11.870130000	-0.144310000	4.212090000
C	10.713920000	0.817090000	3.907760000
C	14.889090000	-0.132790000	2.056050000
O	15.995150000	4.607810000	4.199380000
O	15.785730000	0.800150000	6.214970000
C	15.208400000	1.302190000	5.360840000
C	15.327730000	3.675550000	4.103070000
O	12.376160000	3.378790000	6.071000000
O	9.648550000	1.906540000	2.141490000
O	10.603450000	-0.079950000	1.684840000
C	16.465920000	1.543390000	1.789180000
C	13.057500000	2.902500000	5.263860000
C	10.339390000	0.802180000	2.453010000
C	9.305290000	2.094210000	0.737410000
H	11.613030000	-1.063710000	3.929500000
H	9.982570000	0.481040000	4.387660000
H	10.029130000	1.707350000	0.167210000
H	17.159370000	-0.982400000	-0.083610000
H	16.748310000	2.337440000	1.989830000
H	10.944940000	1.822530000	4.297370000
H	11.997330000	-0.149050000	5.200320000
H	15.212040000	-1.720900000	0.936390000
H	17.900270000	1.097580000	0.367870000
H	13.224710000	-1.375370000	2.441310000
C	9.165130000	3.582730000	0.518360000
H	8.948540000	3.739910000	-0.468200000
H	8.407910000	1.531200000	0.551800000

H	10.037420000	4.099000000	0.685570000
H	8.330530000	3.983820000	0.969830000

Table S7. Cartesian coordinates of **2** at the ZORA/BP86/TZ2P level of theory.

C	3.540720000	1.154300000	0.415586000
C	1.720350000	2.515880000	1.877210000
C	4.242270000	3.410720000	1.675490000
C	6.569080000	1.247900000	2.640460000
H	6.652020000	2.228660000	2.181820000
C	7.704260000	0.549712000	3.053010000
H	8.683240000	1.000360000	2.911650000
C	7.561850000	-0.707925000	3.637970000
H	8.431270000	-1.271320000	3.968930000
C	6.278900000	-1.230890000	3.789250000
H	6.110830000	-2.207350000	4.236850000
C	5.185660000	-0.479521000	3.353170000
C	3.826640000	-0.959974000	3.459350000
H	3.640130000	-1.942110000	3.896370000
C	1.493390000	-0.756345000	3.173360000
H	1.570690000	-1.791420000	3.539890000
C	0.681854000	0.040691000	4.189310000
H	0.793363000	1.121200000	4.040610000
H	-0.382426000	-0.192677000	4.049850000
C	1.057540000	-0.309814000	5.615450000
C	0.787669000	0.318040000	7.888730000
H	0.383471000	-0.655830000	8.184590000
H	0.283355000	1.124720000	8.423850000
H	1.866720000	0.345920000	8.073740000
C	0.769827000	-0.869609000	1.820420000
C	0.969058000	-1.669740000	-0.402991000
H	0.123350000	-2.357800000	-0.304081000
H	1.763840000	-2.114420000	-1.003930000
H	0.633564000	-0.723557000	-0.839218000
Cl	3.421110000	2.521560000	4.616280000
N	5.326610000	0.752893000	2.781710000
N	2.857720000	-0.218434000	3.024080000
O	3.610500000	0.826270000	-0.705666000
O	0.678834000	2.992800000	1.657090000
O	4.748800000	4.406630000	1.342020000
O	1.734320000	-1.272390000	5.946720000
O	0.517047000	0.566928000	6.480710000
O	-0.395045000	-0.563927000	1.640530000
O	1.568860000	-1.431850000	0.903905000
Re	3.451060000	1.750980000	2.227720000

Table S8. Cartesian coordinates of **3** at the ZORA/BP86/TZ2P level of theory.

Re	15.248030000	1.778120000	13.296640000
C	14.537110000	6.532510000	11.316700000
H	13.572030000	6.940790000	11.612250000
C	15.246570000	5.729520000	12.210340000
H	14.843540000	5.537520000	13.201840000

H	19.529500000	-2.035830000	11.313680000
O	15.515300000	1.231570000	16.325840000
O	12.990000000	3.806820000	13.864050000
N	15.316680000	1.942430000	11.116970000
N	16.803520000	0.381250000	12.651580000
N	16.949770000	3.239780000	13.420210000
N	17.917590000	2.851770000	14.240510000
N	18.883290000	3.768560000	14.158460000
C	15.074520000	6.834030000	10.062810000
O	13.046220000	-0.382500000	13.175230000
H	14.525240000	7.473410000	9.372930000
C	14.474510000	2.706460000	10.388980000
H	13.752570000	3.290160000	10.952580000
C	14.509680000	2.752880000	9.001060000
H	13.799540000	3.381060000	8.468770000
C	15.459530000	1.987800000	8.325730000
H	15.518520000	2.001580000	7.238960000
C	16.327080000	1.192570000	9.066710000
H	17.063780000	0.576180000	8.559800000
C	16.235370000	1.174830000	10.462190000
C	17.068610000	0.316190000	11.315970000
C	18.053020000	-0.544880000	10.819030000
H	18.254900000	-0.586940000	9.752650000
C	18.768010000	-1.356740000	11.692800000
C	13.858430000	3.059760000	13.660900000
C	18.485320000	-1.288150000	13.056920000
H	19.010490000	-1.908310000	13.779740000
C	17.504900000	-0.406690000	13.493700000
H	17.256770000	-0.318120000	14.547220000
C	20.086610000	3.630560000	14.973040000
H	20.203330000	4.512240000	15.611570000
H	20.963450000	3.519380000	14.326320000
H	19.963700000	2.739420000	15.592660000
C	18.554770000	4.752590000	13.288530000
H	19.187660000	5.609280000	13.096100000
C	17.300240000	4.423540000	12.807010000
C	16.498390000	5.207680000	11.851040000
C	17.038620000	5.525320000	10.594120000
H	18.016840000	5.134980000	10.314300000
C	16.328840000	6.332970000	9.705370000
H	16.760050000	6.577350000	8.735790000
C	13.874430000	0.426790000	13.212230000
C	15.399740000	1.462170000	15.194080000

Table S9. Cartesian coordinates of **4** at the ZORA/BP86/TZ2P level of theory.

Re	1.408448960	3.496295850	9.524621950
C	2.681933990	4.427954790	10.644330590
H	3.688703030	9.580031550	11.371750000
C	4.359258960	8.369978230	9.714996650
C	3.403268320	8.857519040	10.608585510
H	4.742360410	7.057511040	8.046443610

C	3.994353380	7.443893620	8.738570130
H	5.391868020	8.709036320	9.779050350
O	-0.923720880	5.263768020	10.506864770
O	0.900345650	1.630489810	11.934814130
O	3.484517070	4.880573410	11.350116250
C	-0.019923980	4.620688480	10.153892220
N	2.829942760	2.114487060	8.605203770
N	0.211408540	2.212306780	8.227957390
C	2.668093160	6.990942890	8.651039750
C	1.709691530	7.497670800	9.541685800
H	0.670776110	7.185911870	9.457367510
C	1.091536140	2.322657290	11.025678000
C	2.323219370	1.185713530	7.745106970
C	0.866688640	1.223813360	7.555835660
C	-1.129921420	2.299163820	8.107368880
H	-1.608324550	3.100183310	8.663580160
C	-1.874827840	1.420315230	7.331544600
H	-2.955017720	1.535228640	7.278281320
C	-1.213026790	0.401812040	6.646386060
H	-1.764516300	-0.312001800	6.037200680
C	0.169745510	0.307627040	6.762088470
H	0.703774060	-0.483981480	6.244295430
C	3.159573250	0.260393580	7.111595080
H	2.742834370	-0.475146320	6.429626770
C	4.527874340	0.279809030	7.358557960
H	5.185071130	-0.439091880	6.872681250
C	5.037160990	1.231832440	8.241715650
H	6.098582990	1.285268550	8.472834210
C	4.159515710	2.126336490	8.840289000
H	4.514400930	2.879452770	9.538365320
N	1.788389190	4.775978320	7.733341700
N	1.594957490	4.218730560	6.544628810
N	1.977804200	5.112933160	5.631604010
C	1.900659300	4.787992570	4.198913860
H	1.625253770	3.728089520	4.157904900
H	2.911988960	4.898669820	3.787675890
C	0.900299080	5.652511140	3.424744110
H	1.181684820	6.711978090	3.522745110
H	1.035067040	5.401595030	2.361948210
C	-0.559989600	5.444876970	3.832464940
H	-0.868588440	4.400273260	3.683027450
H	-1.221241830	6.078892320	3.228488300
H	-0.729229930	5.700779390	4.887696150
C	2.419995210	6.252281190	6.218111200
H	2.763877060	7.113087230	5.659679420
C	2.300050730	6.048319020	7.580179350
C	2.079145660	8.423030300	10.517169170
H	1.327143150	8.811000710	11.202088060

Table S10. Cartesian coordinates of **5** at the ZORA/BP86/TZ2P level of theory.

Re	6.754697000	1.531667000	4.223235000
Cl	8.471440000	3.289339000	4.464830000
N	6.711526000	2.293576000	8.415085000

N	6.945718000	1.411210000	6.371191000
O	4.500169000	-0.578525000	4.092694000
O	8.835418000	-0.621563000	3.469237000
O	6.217440000	2.302343000	1.281327000
C	7.677661000	0.644185000	7.246549000
C	8.464993000	-0.490423000	7.025619000
H	8.582734000	-0.898294000	6.025382000
C	9.083502000	-1.058622000	8.133583000
H	9.703413000	-1.943547000	8.002812000
C	8.929711000	-0.515258000	9.429283000
H	9.430360000	-0.994842000	10.268467000
C	8.152234000	0.617403000	9.660330000
H	8.032200000	1.030709000	10.660542000
C	7.532319000	1.185604000	8.544471000
C	6.368256000	2.384068000	7.088169000
C	5.481137000	3.304921000	6.408520000
C	4.689564000	4.296573000	7.003096000
H	4.708138000	4.451200000	8.075316000
C	3.855292000	5.077753000	6.209639000
H	3.237092000	5.850543000	6.663752000
C	3.820086000	4.849514000	4.832535000
H	3.185094000	5.435523000	4.171937000
C	4.617637000	3.841519000	4.303657000
H	4.625634000	3.619085000	3.239950000
N	5.428344000	3.076142000	5.057167000
C	6.333015000	3.154563000	9.529141000
H	6.353849000	4.194094000	9.182106000
H	7.128199000	3.057145000	10.278014000
C	4.981484000	2.769009000	10.130473000
H	4.734075000	3.440794000	10.964555000
H	5.016381000	1.737364000	10.505623000
H	4.183490000	2.830804000	9.378048000
C	5.356636000	0.215975000	4.142806000
C	8.048997000	0.198982000	3.727583000
C	6.455536000	1.980042000	2.376239000